# The $Q$ value for the $^{26}Al^m$ superallowed beta decay

S. A. Brindhaban and P. H. Barker
*Physics Department, Auckland University, Auckland, New Zealand*
(Received 18 January 1994)

The threshold energy of the $^{26}Mg(p,n)^{26}Al^m$ reaction has been measured to be 5209.46±0.12 keV, using a 1 V standard as reference, and taking account of effects due to finite beam energy spread, nonuniform proton energy loss in the target, and ionization of the magnesium atoms. The $Q$ value derived for the $^{26}Al^m$ beta decay then becomes 4232.17±0.12 keV, which is in clear disagreement with the most precise of the existing measurements. A further measurement is proposed.

PACS number(s): 21.10.Dr, 23.40.−s, 27.30.+t, 24.80.Dc

## I. INTRODUCTION

As pointed out by Hardy *et al.* [1], and reemphasized recently [2], the study of superallowed $0^+$ to $0^+$, $T = 1$ Fermi beta decays continues to be of fundamental interest. The knowledge of the strengths of these transitions provides both a precise test of the conserved vector current hypothesis and of the three-generation standard model, and, in addition, when combined with parameters from the decay of the neutron, a means of ascertaining the sizes of the weak interaction coupling constants $G_V$ and $G_A$ individually.

Of the decays whose strengths, or $ft$ values, may possibly be measured with a precision approaching 0.1%, eight are discussed in [1], although a ninth, that of $^{10}C$, should not be ignored, despite being experimentally more difficult [3]. For all nine decays, establishing the magnitude of the $ft$ value involves measuring three parameters, the decay energy, the half-life, and the branching ratio. Each of these has its own attendant difficulties. The present work describes the determination of decay energies, and in particular that of $^{26}Al^m$.

The data compilation discussed in [1] shows that there have been four groups who have tried to measure the $Q$ values for several of the superallowed decays with a precision of better than 0.5 keV. The first, whose method and results are described by Vonach *et al.* [4], determined the ingoing and outgoing particle energies in ($^3$He,$t$) reactions, with the ultimate energy reference being a time-of-flight system over more than 100 m. So that, for instance, the $^{26}Al(\beta^+)^{26}Mg$ decay energy was given directly in terms of the $^{26}Mg(^3He,t)^{26}Al$ $Q$ value. The second, of Koslowsky *et al.* [5], was somewhat similar, but determined the differences between pairs of decay energies by looking simultaneously at the outgoing particles from pairs of ($^3$He,$t$) reactions, and so ultimately relied on other determinations to establish an absolute energy scale, although not of course to test the conserved vector current hypothesis. The third looked at the difference, in three cases, of the proton separation and neutron separation energies of the decaying nucleus via the determination of $(p,\gamma)$ and $(n,\gamma)$ $Q$ values, Kikstra *et al.* [6]. This technique has more steps involved than the others. For example, for the $^{26}Al^m$ decay, first some narrow resonances in the $^{25}Mg(p,\gamma)^{26}Al$ reaction were chosen, and their proton energies measured relative to the energy of a resonance in the $^{27}Al(p,\gamma)^{28}Si$ reaction. Then, in a second step, the excitation energies in the nucleus $^{26}Al$ fed by the resonances were established by comparing the energies of their deexcitation gamma rays with those of gamma ray standards. And finally, in a third experiment, the excitation energy within $^{26}Mg$ fed by thermal neutrons was compared with that from other neutron capture reactions. The fourth method, of which the present work is an example, is most recently described in Brindhaban *et al.* [7]. Here the threshold energy for a $(p,n)$ reaction is measured fairly directly in terms of a 1 V standard, so that for $^{26}Al^m$, what will be described is the acquisition of a yield curve of the reaction $^{26}Mg(p,n)^{26}Al^m$, as a function of incoming proton energy. The proton energy at threshold then provides the $^{26}Al^m$ decay energy directly.

The most important joint feature of the four techniques described above is that they differ from one another in many of their aspects. Thus many of their intrinsic sources of error should be different, which is important when the experiments being attempted are near the limit of what is currently possible. If there is good agreement between several of them, one can then place some reliance on the conclusions drawn. For the $^{26}Al^m$ decay, it can be seen from Ref. [1] that the overall situation is not reassuring. Indeed the quoted "average" value is completely incompatible with the most precise one from Ref. [6].

Accordingly, we describe here the determination of the threshold energy, at around 5210 keV, of the $^{26}Mg(p,n)^{26}Al^m$ reaction, and the absolute calibration of that energy in terms of a maintained 1 V standard using a beam of surface-ionized $^{133}Cs^+$ accelerated between ground potential and 39.6 kV. This threshold has been studied twice previously, with moderate precision, in techniques which relied for their energy scale on a comparison with alpha particles from radioactive sources, and once in Auckland using an earlier form of the present system [8]. As the present technique is somewhat unusual, we try to expose the various parts of it in detail since, although several aspects have been recently improved [9], we have not discussed the whole system for some time [10].

 

## II. ENERGY MEASUREMENT: HISS

The method for the measurement of the mean kinetic energy of the proton beam used in the $(p,n)$ reaction, and of the energy distribution is via a heavy ion source system (HISS) and is simple. The proton beam from the AURA2 tandem accelerator at the University of Auckland passes on a tightly collimated path around an Enge split-pole magnetic spectrograph. Then, without altering the magnetic field, a beam of $^{133}Cs^{+}$ ions is accelerated through a voltage difference $V$ to pass along the same path. The size of $V$ is determined using a purpose-built fixed-ratio resistive divider (the HVD), and then a variable-ratio commercial Kelvin-Varley divider (the KVD), whose output is compared with one volt using a microvoltmeter. Thus a kinetic energy of 5.21 MeV is determined with three successive divisions. First (mass of $^{133}Cs^{+}$)/(mass of proton) to give 39.6 kV. Second a fixed ratio of 10 001 from the HVD to give 3.96 V, and third a ratio of 0.252 from the KVD to give 1 V. Of course, if one is aiming for a precision of better than 10 ppm, each one of these seemingly simple steps involves additional features at levels which are not negligible, but as will appear, none is greater than 50 ppm, and we believe each is understood at a level of 3 ppm or better. We illustrate the above by taking one particular calibration and yield point and following the calculation of the proton mean energy.

The "standard" spectrograph geometry is to collimate with object and image slits of widths 0.075 and 0.025 mm, respectively. In addition, the entrance angles are constrained by a rectangular set of slits, $0.8\times0.8$ mm$^2$, 170 mm downstream of the object point. As shown in Ref. [9], this leads to an emerging beam of Gaussian energy distribution with a full width at half maximum, (FWHM), of 55 ppm, which is entirely brought about by the sizes of the object and image slits. The effect of aberrations caused by finite entrance angles is negligible. To increase the yield of the present experiment we departed from this ideal situation, and opened out the collimation. As indicated in Ref. [9], this was effected, not by widening the entrance angles which would eventually have led to principally second order, and nonsymmetric, aberration effects, but by opening the object and image slits. Figure 1 shows a transmission curve for $^{133}Cs^{+}$ ions accelerated through about 39.6 kV, measured as a current, as the accelerating voltage was varied over a small range. The object and image slit sizes were 0.09 and 0.03 mm, respectively. As can be seen the energy shape is a symmetric, slightly "flattened" Gaussian, with a FWHM of 75 ppm and a center at $-19(2)$ ppm. An important feature to emphasize here is that, because this shape is entirely understood in terms of the sizes of the object and image slits, it may be safely inferred that it represents also the shape of a transmitted proton beam, with identical central momentum.

To use Fig. 1 as a calibration for a subsequent proton energy, some additional parameters need to be noted. The magnetic field is monitored with a nuclear magnetic resonance (NMR) probe whose output is locked onto the field. For this measurement its frequency was 26.016 92 MHz, which remained constant to better than 1 ppm. The spectrograph nominal temperature was 18.8 °C. The KVD ratio was 0.252 572 7. The calibration parameter, or $X$ value, which is derived as follows, is conveniently taken to be proportional not to the particle momentum, $p$, but to $p^2$, and can be expressed nonrelativistically as [(mass)×(kinetic energy)]/(NMR frequency)$^2$. The mass of a $^{133}Cs^{+}$ ion is [11] 132.905 433 u−0.000 549 u=132.904 88 u. To obtain the accelerating voltage we note that the HVD ratio of 10 001 is actually a slight function of applied voltage. This has been thoroughly investigated and the ratio at 39.6 kV is 10 000.44(3). Hence, taking the central position of $-19(2)$ ppm, the accelerating voltage is $(1.000\,000/0.252\,572\,7)\times10\,000.44\times(0.999\,981)$=39.593 55 kV. This does not give the kinetic energy directly because there is a small contact potential between the metal surface of tungsten where the cesium atoms are ionized and the average of the spectrograph internal metal surfaces between which an ion flies, and which defines zero electrostatic potential for it. This contact potential is measured in a series of sepa-

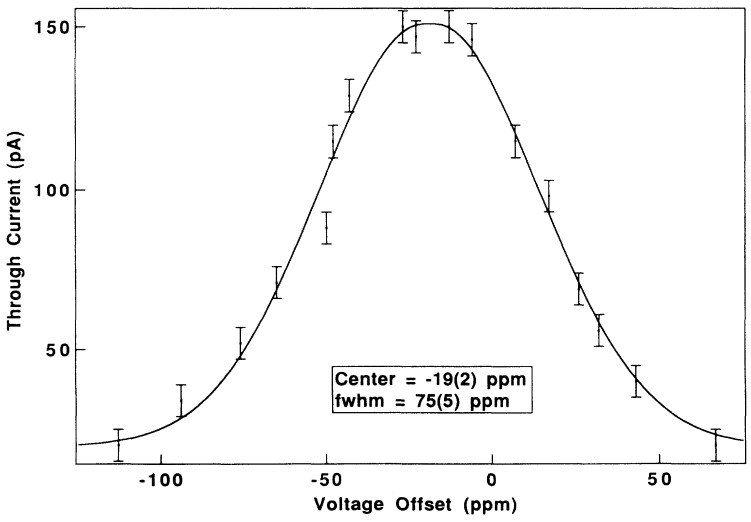


FIG. 1. A calibration scan of $^{133}Cs^{+}$ ions showing the symmetric energy profile with center at $-19(2)$ ppm and FWHM of 75 ppm.

rate experiments for each new surface, and was for this case $-0.9(1)$ eV. Hence the mean ion kinetic energy was $39\,593.55-0.9 = 39\,592.65$ eV and thus the calibration $X$ value was $132.904\,88\times39.592\,65/(26.016\,92)^2 = 7773.986$ in units of u eV/MHz$^2$. A last, small, factor is that, as discussed in [9], the momentum selected is slightly dependent, with a linear coefficient of +33(3) ppm/C, on the spectrograph nominal temperature, which is monitored via a resistance thermometer buried in the aluminum casing. Consequently, all $X$ values are normalized to 25 °C and $X$ becomes $7773.986\times(1+6.2\times0.000\,033)=7775.58$. This last step is not as large as it might seem, since the experiments are invariably done within less than 1 °C of the calibrations.

The assigned error to $X$ is composed partly of elements, such as those from the NMR frequency or determining the center of the scan, whose influence would decrease with repeated scans, and others, such as from the contact potential and the nonconstancy of the 100 001 ratio, which would not. So for each $^{26}Mg(p,n)^{26}Al^m$ yield curve, the difference between the prior and post calibrations will be included in the error assigned to the threshold value, and then the systematic errors, of certainly less than 10 ppm, will be included in the final mean value.

Although a calibration was performed immediately before and after each yield curve run, it was not always a complete scan, as the amount of cesium adsorbed on the ion source was limited, and a technique which used much less was to locate the maximum of the scan in terms of the acceleration voltage offset. Experience has shown that five or six sequential locations of the maximum are more than equivalent in reliability to a full scan, and the saving in cesium is substantial.

## III. YIELD MEASUREMENTS

After passing through the spectrograph image slit, the proton beam traveled 60 cm further before striking the target perpendicularly over a rectangular area roughly 1 cm high and 0.5 cm wide. The intensity of the beam never exceeded 150 nA, and the targets were evaporated metallic $^{26}Mg$, enriched to 80%, 10–15 keV thick to the proton beam, transported in argon from the evaporator, and exposed for a few seconds to air.

The yield of the $^{26}Mg(p,n)^{26}Al^m$ reaction was monitored by detecting the positrons emitted by the $^{26}Al$ nuclei, of maximum energy 3.2 MeV, using a plastic scintillator $dE$-$E$ telescope placed just behind the target, but outside the vacuum. To be counted, a positron had to pass through the target backing (0.125 mm Ta), then through a stainless-steel window of 0.075 mm, through the 0.9 mm plastic $dE$ detector and then register in the 3 cm thick plastic $E$ detector. A $dE$-$E$ 10 ns coincidence requirement retained the positron signal while reducing background by a large factor.

The reaction energies for a yield curve were chosen by keeping the spectrograph magnetic field, and hence the proton kinetic energy, constant via the NMR signal, and applying an offset voltage difference between the target and ground. Each yield was evaluated as follows. The proton beam was allowed to strike the target for 20 s, after which it was shut off by a tantalum plate 5 m upstream of the spectrograph. After a delay of 0.1 s, the time decay of the logic output of the telescope was followed for 20 s in a 512 channel multiscalar after which, following a further 0.1 s delay, the beam was allowed through again. Thirty such decays were accumulated for each point of a yield curve such as the one shown in Fig. 2. The actual yield was then calculated by analyzing this decay curve in terms of a constant plus an exponential decay whose half-life was that of $^{26}Al^m$, 6.34 s. The amplitude of this decay was then the yield.

To monitor the number of protons which had struck the target, a small collimated silicon semiconductor detector registered protons scattered from the target at roughly 140° to the incoming beam. Hence the normalized yield was the decay amplitude mentioned above divided by this number.

A minor complication was that it seemed impossible to make magnesium targets as described without introducing a small amount of sodium contaminant. This pro-

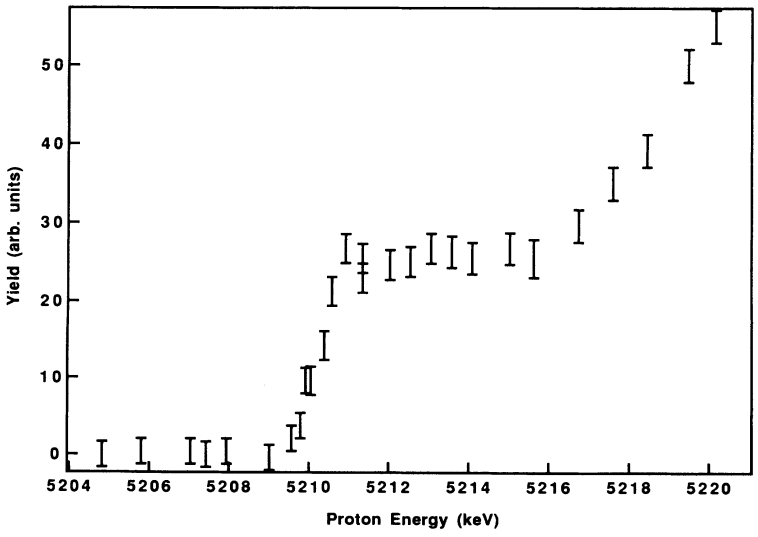


FIG. 2. An exploratory yield curve of $^{26}Mg(p,n)^{26}Al^m$.

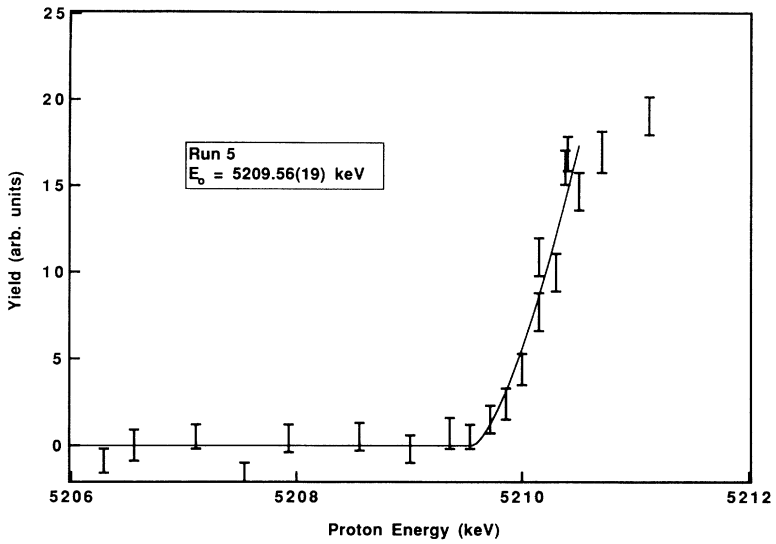


FIG. 3. The yield curve of $^{26}Mg(p,n)^{26}Al^m$ taken for run 5 of Table I.

duced $^{23}Mg$, with half-life 11.6 s and maximum positron energy 3.1 MeV, and it was identified in terms of this half-life. To include its effects in the analysis, several lengthy runs were performed a few keV below the threshold for $^{26}Al^m$, and the normalized yield of the $^{23}Mg$ ascertained. Then, with the assumption that this yield was sufficiently constant over a proton energy range of 5 keV, a suitable decay curve was subtracted from the $^{26}Al^m$ yield curves before they were analyzed. This correction, however, was very small, and had the effect, for the yields of Fig. 3, of contributing on average 0.15.

To illustrate the calculation of the reaction energy for a particular yield point we choose the point in Fig. 3 which is at approximately 5210.5 keV. The associated parameters are NMR frequency 26.014 95 MHz, spectrograph temperature 18.3 °C, target voltage −1850 V. The mean $X$ value before and after the run was 7775.50. So the nonrelativistic proton kinetic energy is $E_{nr} = (Xf^2/m_p) = 5224.267$ keV, with the proton mass, $m_p$, taken as 1.007 277 u. In this case, however, a relativistic calculation is necessary, and this is given by $E = -m_p + m_p(1 + 2E_{nr}/m_pc^2)^{1/2}$=5209.80 keV. Correction up to 18.3 °C gives 5208.65 keV, and including the voltage offset gives a final reaction energy of 5210.50 keV.

## IV. ANALYSIS

Seven yield curves were taken as described above, the first one exploratory over a wide energy range, and the others for detailed analysis, each of these last being with a freshly prepared $^{26}Mg$ target and with independent $X$ calibrations performed immediately before and after. The data of Fig. 2 illustrate the particular idiosyncrasy of this reaction, namely the pronounced resonance in the yield within a few keV of threshold, which we had noted in Ref. [8]. In that work an analysis had been barely possible, and that only by adding together five separate yield curves. Since then the use of the positron telescope, coupled with the time analysis of its output, as outlined above, has meant that the yield curves, such as the one in Fig. 3, are considerably improved. In that figure, the continuous line is the fit to the data in terms of the function $Y = A + B(E - E_0)^{3/2}$, where $E_0$ is the threshold energy, which is the expected form of the thick target yield of $s$-wave neutron emission. It should be emphasized that only the data up to a proton energy of 5210.5 keV, i.e., within 1 keV above the threshold, have been used in the analysis, and that this was the case for all six runs. The six yield curves were analyzed thus using non-

TABLE I. Parameters for each $^{26}Mg(p,n)^{26}Al^m$ threshold run. The FWHM of the proton beam, the raw extracted threshold, the corrections for the finite beam FWHM ($\Delta_f$), for the nonuniform proton energy loss ($\Delta_q$) and for atomic ionization ($\Delta_{at}$), and the final threshold energies (all in keV).

| Run | FWHM | $E_0$ (raw) | $\Delta_f$ | $\Delta_q$ | $\Delta_{at}$ | $E_0$ (final) |
|---|---|---|---|---|---|---|
| 1 | 0.60 | 5209.24(13) | 0.09 | 0.06 | −0.10 | 5209.29(14) |
| 2 | 0.60 | 5209.66(23) | 0.09 | 0.06 | −0.10 | 5209.71(24) |
| 3 | 0.60 | 5209.47(12) | 0.09 | 0.06 | −0.10 | 5209.52(13) |
| 4 | 0.39 | 5209.55(18) | 0.04 | 0.06 | −0.10 | 5209.55(19) |
| 5 | 0.39 | 5209.56(19) | 0.04 | 0.06 | −0.10 | 5209.56(20) |
| 6 | 0.39 | 5209.65(36) | 0.04 | 0.06 | −0.10 | 5209.65(36) |

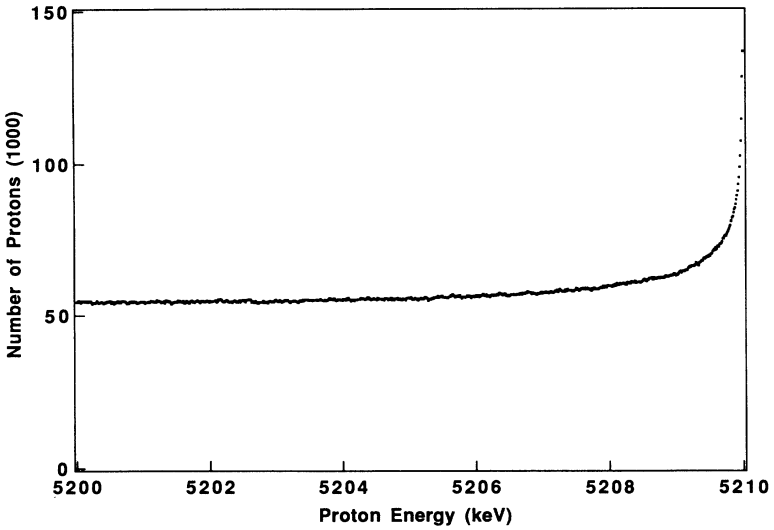


FIG. 4. The energy distribution of a beam of protons, of initial energy 5210 keV, inside a target of $^{26}Mg$, according to a $1/q^2$ energy loss dependency.

linear least squares optimization, and the values of $E_0$ extracted. The results are summarized in Table I, which also contains information on the FWHM of the proton beam energy. Because of the way in which the yield is calculated, as described in Sec. III, the value of the coefficient $A$ should be consistent with zero. This was true in all six cases.

The functional form above assumes that the proton beam energy width is infinitesimal, that the protons lose energy uniformly as they slow down in the target, and that the atoms which are involved in the nuclear reaction are not ionized. Each of these factors has to be understood and corrected for, and the procedures adopted were the following. The proton beam energy distribution is known, as discussed above, that appropriate to runs 4–6, with a FWHM of 75 ppm (=0.39 keV) being shown in Fig. 1. Accordingly, an artificial yield curve was generated in steps of 10 eV up to 10 keV above threshold. This was then convoluted with the distribution of Fig. 1, using the techniques of fast Fourier transforms, and the resulting curve analyzed, up to approximately 1 keV above threshold, in terms of $(E - E_0)^{3/2}$. The shift in the value of $E_0$ was taken to be the correction to be applied for this effect.

Nonuniform proton energy loss in the target was dealt with similarly. As a proton slows down by colliding with electrons, the probability of losing energy $q$ in a collision is proportional to $1/q^2$, with a maximum $q, q_{max}$, given by a head-on classical collision, and a minimum, $q_{min}$, taken to be $I^2/q_{max}$, with $I$ the ionization energy. So an energy profile of the protons in the target at any time will not be flat, but rather will have an excess of higher energy particles, as illustrated in Fig. 4. This curve was generated in a straightforward way using Monte Carlo methods. To establish the effects of this on a yield curve, it was convoluted with the cross-section dependency $(E - E_0)^{1/2}$ in 10 eV steps over 10 keV and the result analyzed as above. [The $(E - E_0)^{3/2}$ dependency is obtained by convoluting with the flat distribution.]

The third effect, that of ionization of the target atom of a nucleon undergoing the $(p, n)$ reaction, has been treated recently [12]. Briefly, a perturbative approach gave the differential probability $dP/dE$ for a proton to lose energy $E$ by expelling an electron out of a particular subshell

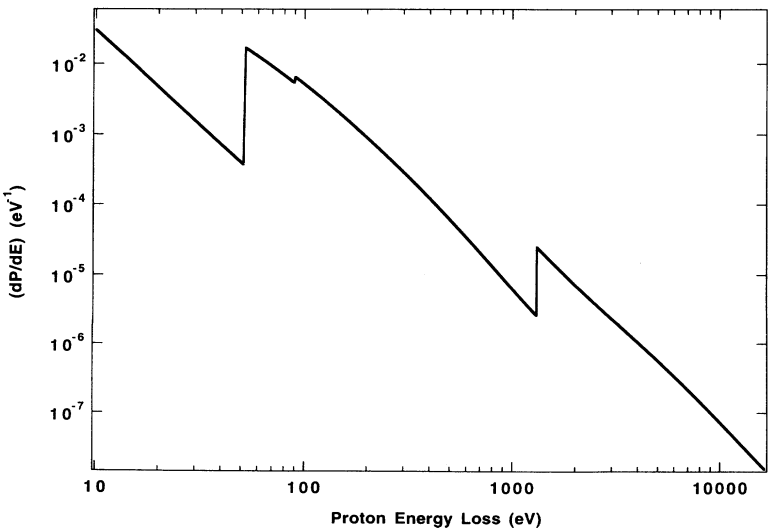


FIG. 5. Energy loss distribution of 5210 keV protons to electrons ejected from $^{26}Mg$ atoms during a $(p, n)$ reaction.

during the $(p,n)$ reaction. Summing these subshell probabilities in 10 eV steps gave the total curve of Fig. 5, which was then convoluted with the $(E-E_0)^{3/2}$ form and analyzed to find the threshold shift.

The sizes of these corrections and their effects on the raw extracted thresholds are shown in Table I, which also contains for each run a 10 ppm contribution to the assigned error due to the uncertainty in the mean $X$ value. A corroboration of the magnitude of the calculated correction for ionization, the third effect considered, can be obtained by noting that the mean energy loss, derived directly from Fig. 4 (which is a crude estimate of the total shift of the yield curve) is 135 eV.

## V. RESULTS

The weighted mean threshold value from Table I is 5209.49(7) keV, with a $\chi^2$ of 4 from 6 points. Also to be included is a possible 10 ppm systematic error from the HISS energy measuring process. An electrical effect in the HVD, whose presence was realized after the calibration scans had been performed, reduces the energies by 6 ppm. And finally the estimated errors incurred in the procedures for calculating the three corrections discussed in Sec. IV are assigned sizes of half their magnitude. The final threshold value therefore becomes 5209.46(12) keV, which is preferred over the preliminary value from the same data cited in Ref. [7], which it replaces, mainly because the corrections for nonuniform proton energy loss and for atomic ionization have been more thoroughly investigated and included. We would also like it to replace the result of 5208.86(23) keV from our laboratory, quoted in the conference proceedings of Ref. [8], with which it is, however, not in serious disagreement. But the data for the latter were somewhat inadequate, as discussed above, and accordingly they were never published in a journal.

From this figure, the $Q$ value for the $^{26}\mathrm{Mg}(p,n)^{26}\mathrm{Al}^m$ reaction becomes 5014.57(12) keV, and the $Q$ value for the positron (actually the electron capture) decay of $^{26}\mathrm{Al}^m$ becomes 4232.17(12) keV, using 782.40 keV for the mass difference of the hydrogen atom and the neutron. This $Q_{ec}$ is in good agreement with the compilers' mean value of 4232.01(18) keV, quoted in Ref. [1]. But, as noted above, it is in poor agreement with the most precisely quoted value, namely 4232.81(10) keV from Ref. [6]. A further interesting comparison is with the $Q$-value difference from the Chalk River ($^3$He,$t$) studies, $Q_{ec}(^{26}\mathrm{Al}^m) - Q_{ec}(^{14}\mathrm{O})$=1401.68(13) keV, Ref. [1]. The comparable figure for results from Auckland (from Ref. [13]) is 4232.17(12) keV $-2830.31(8) = 1401.86(14)$ keV, although it should be pointed out that the $^{14}$O result does not contain corrections as discussed above. But they would be unlikely to affect the $Q$ value by more than 100 eV.

## VI. DISCUSSION

The beta decay $Q$ value for the pure Fermi transition of the nucleus $^{26}\mathrm{Al}^m$ to its $0^+$, $T=1$ partner in $^{26}$Mg has been measured by determining the threshold energy for the associated $(p,n)$ reaction, using a method which relates the absolute energy calibration fairly directly to a 1 V standard. The result obtained, although in accord with the presently accepted value, is in disagreement with the presently most precisely quoted value, which is based on a method of comparison of $(p,\gamma)$ and $(n,\gamma)$ $Q$ values. It does not seem worthwhile therefore to draw conclusions at a high level of precision about the $ft$ value of the $^{26}\mathrm{Al}^m$ decay until this difference is explored. Accordingly, we aim to attempt to repeat the latter measurement, at least for the $(p,\gamma)$ part, using our ability to measure proton resonance energies directly, and measuring deexcitation gamma-ray energies relative to known standards.

## ACKNOWLEDGMENTS

We would like to thank the technical staff of the AURA2 tandem laboratory, M. J. Keeling and W. B. Wood, for their enthusiastic assistance and support. In addition, we warmly acknowledge the support of the University of Auckland Research Grants Committee. One of us (P.H.B.) is extremely grateful to the Istituto Nazionale di Fisica Nucleare, Sezione di Firenze at the Dipartimento di Fisica, Università di Firenze for their warm hospitality during the final stages of this work.

[1] J. C. Hardy, I. S. Towner, V. T. Koslowsky, E. Hagberg, and H. Schmeing, Nucl. Phys. **A509**, 429 (1990).

[2] International Workshop on Symmetry Tests in Nuclei, June 1993, Louvain-La-Neuve (unpublished).

[3] M. A. Kroupa, S. J. Freedman, P. H. Barker, and S. M. Ferguson, Nucl. Instrum. Methods **A310**, 649 (1991).

[4] H. Vonach, P. Glässel, E. Huenges, P. Maier-Komor, H. Rösler, and H. J. Scheerer, Nucl. Phys. **A278**, 189 (1977).

[5] V. T. Koslowsky, J. C. Hardy, E. Hagberg, R. E. Azuma, G. C. Ball, E. T. H. Clifford, W. G. Davies, H. Schmeing, U. J. Schrewe, and K. S. Sharma, Nucl. Phys. **A472**, 419 (1987).

[6] S. W. Kikstra, Z. Guo, C. Van der Leun, P. M. Endt, S. Raman, T. A. Walkiewich, and I. S. Towner, Nucl. Phys. **A529**, 39 (1991).

[7] P. H. Barker and S. A. Brindhaban, in *Proceedings of the 6th International Conference on Nuclei Far from Stability and the 9th International Conference on Atomic Masses and Fundamental Constants*, Bernkastel-Kues, 1992, edited by R. Neugart and A. Wöhr (IOP, Bristol, 1992), p. 777.

[8] P. H. Barker, R. E. White, D. M. J. Lovelock, and R. M. Smythe, *Proceedings of the 7th International Conference on Atomic Masses and Fundamental Constants*, Darmstadt, 1984, edited by O. Klepper (Technische Hochschule, Darmstadt, 1984), p. 55.

[9] P. H. Barker, S. C. Baker, S. A. Brindhaban, and M. J. Brown, Nucl. Instrum. Methods **A306**, 272 (1991).

[10] R. E. White, P. H. Barker, and D. M. J. Lovelock, Metrologia **21**, 193 (1985).

[11] A. H. Wapstra and K. Bos, At. Data Nucl. Data Tables **19**, 175 (1977).

[12] P. A. Amundsen and P. H. Barker, submitted to Phys. Rev. C.

[13] R. E. White, H. Naylor, P. H. Barker, D. M. J. Lovelock, and R. M. Smythe, Phys. Lett. **105B**, 116 (1981).